Contents lists available at ScienceDirect

Digital Chinese Medicine

journal homepage: http://www.keaipublishing.com/dcmed

Facial and tongue features in traditional Chinese medicine for coronary artery stenosis warning and their association chain with cardiac biomarkers

Yu Wang[a, b], Pengcheng Ding[c], Zhentao Li[a], Jiyu Zhang[a], Liping Tu[d], Jijie Xu[e*], Jiatuo Xu[a*]

a. School of Traditional Chinese Medicine, Shanghai University of Traditional Chinese Medicine, Shanghai 201203, China

b. Production Technology Department, Wuhu Shengmeifu Technology Co., Ltd., Wuhu, Anhui 241005, China

c. Digital and Intelligent Health Research Center, Anqing Normal University, Anqing, Anhui 246133, China

d. School of Artificial Intelligence in Traditional Chinese Medicine, Shanghai University of Traditional Chinese Medicine, Shanghai 201203, China

e. Department of Cardiology, Shanghai Baoshan Hospital of Integrated Traditional Chinese and Western Medicine, Shanghai 201999, China

A R T I C L E I N F O

Article history
Received 09 December 2025
Accepted 21 April 2026
Available online 25 June 2026

Keywords
Tongue diagnosis
Facial diagnosis
Coronary heart disease (CHD)
Risk warning model
Partial least squares structural equation modeling (PLS-SEM)

A B S T R A C T

Objective To explore whether digital facial and tongue diagnostic technologies can support the assessment of coronary heart disease (CHD) patients for coronary artery stenosis severity, and examine potential associations between digital tongue diagnosis features and myocardial biomarkers.

Methods The TFDA-1 face and tongue diagnosis instrument and the TDAS analysis system were used to perform intelligent visual examination and analysis of the facial and tongue in CHD patients who attended the Department of Cardiology at Shanghai Baoshan Hospital of Integrated Traditional Chinese and Western Medicine between October 2, 2023 and July 31, 2024. Variables were screened using principal component analysis (PCA) and multicollinearity analysis to construct four machine learning models, including random forest, LightGBM, decision tree, and naive Bayes, for the early prediction of coronary artery stenosis severity. Model performance metrics, including sensitivity, specificity, precision, F1 score, accuracy, and the area under the receiver operating characteristic (ROC) curve (AUC), were evaluated. Visual analyses were performed using the SHapley Additive exPlanations (SHAP) interpreter and decision curve analysis. For patients after percutaneous coronary intervention (PCI), a conceptual model linking cardiac biomarkers and tongue diagnosis was constructed using the partial least squares structural equation modeling (PLS-SEM), and its validity was assessed.

Results A total of 459 CHD patients were enrolled and assigned to a PCI group and a non-PCI group (which comprised two subgroups: mild stenosis or less group, moderate stenosis or greater group). For sublingual vein (SV) features, the PCI group had lower SV-a and SV-b than the other groups ($P < 0.01$ and $P < 0.05$, respectively). For tongue surface features, the PCI group had significantly higher tongue body (TB)-L, TB-a, and TB-b ($P < 0.05$, $P < 0.01$, and $P < 0.001$, respectively), as well as higher tongue coating (TC)-a and TC-b ($P < 0.01$ and $P < 0.001$, respectively). Age, SV-a, SV-b, creatine kinase-myocardial band (CK-MB), CK, TC-a, lip-L, and lip-b were incorporated in the machine learning models. The random forest model performed best, with an AUC of 0.924, an F1 score of 0.839, precision of 0.807, accuracy of 0.864, sensitivity of 0.873, and specificity of 0.839. Decision curve analysis indicated that both LightGBM and random forest had clinical utility. PLS-SEM confirmed the pathway relationships:

*Corresponding author: Jiatuo Xu, E-mail: xjt@fudan.edu.cn. Jijie Xu, E-mail: adamxu628@163.com.

Peer review under the responsibility of Hunan University of Chinese Medicine.

DOI: 10.1016/j.dcmed.2026.05.007

Citation: WANG Y, DING PC, LI ZT, et al. Facial and tongue features in traditional Chinese medicine for coronary artery stenosis warning and their association chain with cardiac biomarkers. Digital Chinese Medicine, 2026, 9(2): 184-196.

myocardial biomarkers → TB and myocardial biomarkers → TC (coefficient = – 0.238, t = 2.239, P = 0.025, and coefficient = – 0.270, t = 2.522, P = 0.012, respectively).

Conclusion This study developed a noninvasive early warning model for coronary artery stenosis in patients with CHD. It applied PLS-SEM to investigate the association between post-PCI cardiac biomarkers and tongue diagnosis, and validated the proposed association chain. These findings suggest that intelligent traditional Chinese medicine (TCM) visual diagnosis integrated with modern digital technology may support CHD risk assessment and comprehensive health management.

1 Introduction

In recent years, research on coronary heart disease (CHD) has shifted from individual traditional risk factors to a more comprehensive, nuanced evaluation. Coronary angiography (CAG) remains the gold standard for directly visualizing coronary artery anatomy and assessing stenosis severity [1]. However, this conventional diagnostic approach has limitations, including potential trauma and radiation exposure related to vascular access and contrast medium administration [2, 3]. The optimization of non-invasive testing and multiparameter diagnosis has become an important trend in the clinical management of CHD [4–6].

Traditional Chinese medicine (TCM) visual diagnosis techniques based on digital image features may offer a new approach by focusing on localized features and combining them with multidimensional clinical data to establish a simple, convenient, and cost-effective auxiliary diagnostic method for CHD in primary healthcare settings. According to TCM theory, “the tongue is the sprout of the heart” and “the heart manifests its brilliance on the face” [7]. Major disease states, health status, and subtle fluctuations in blood circulation and metabolism induce small color changes in the tongue and facial images that are imperceptible to the naked eye [8, 9]. Previous studies have found that the four diagnostic methods of TCM are useful for predicting and assessing the progression of coronary heart disease [10, 11]. Limited studies have focused on digital features of the tongue and face to construct a model of coronary artery stenosis. Cardiac biomarkers are important for risk stratification and treatment decisions in CHD [12-14]. One study identified significant differences in tongue color associated with varying degrees of myocardial injury [15], and another suggested that tongue features may serve as efficacy indicators reflecting recovery following percutaneous coronary intervention (PCI) [16]. Therefore, the intrinsic association between digital tongue features and cardiac biomarkers may have clinical value for the non-invasive and convenient assessment of patients following PCI.

This study examined the digital features of TCM visual diagnosis that have been overlooked in previous research. It investigated whether digital tongue and facial diagnostic technologies can improve the assessment of CHD, constructed a machine learning model to assess the severity of coronary artery stenosis, and evaluated its clinical decision-making value. The study also used partial least squares structural equation modeling (PLS-SEM) to develop a conceptual model linking post-PCI myocardial biomarkers to tongue features, and to assess its validity through internal and external model evaluation. This study provides an objective basis and methodology for the risk stratification of CHD and post-PCI assessment.

2 Data and methods

2.1 Participants

The study participants were CHD patients admitted to the Department of Cardiology at Shanghai Baoshan Hospital of Integrated Traditional Chinese and Western Medicine from October 2, 2023 to July 31, 2024. This study was conducted in accordance with the Declaration of Helsinki. It was approved by the Ethics Committee of Shuguang Hospital Affiliated to Shanghai University of Traditional Chinese Medicine (Approval No. 2023-2-5-04) and was registered in the Chinese Clinical Trial Registry (ChiCTR1900026008). All participants provided written informed consent.

2.2 Diagnostic criteria and grouping

The diagnostic criteria for CHD were based on the European Society of Cardiology (ESC) [17, 18] and included typical symptoms such as chest pain including paroxysmal angina or compressive pain, diminished heart sounds on auscultation, abnormal ST-segment changes on electrocardiography, and CAG findings showing stenosis in at least one vessel.

Participants were divided into two groups: a non-PCI group and a PCI group. The non-PCI group was further classified into two subgroups based on the severity of stenosis: mild stenosis or less (CAG-assessed luminal stenosis < 50%) and moderate stenosis or greater (CAG-assessed luminal stenosis ⩾ 50%), in accordance with the 2023 ESC Guidelines for the Management of Acute Coronary Syndromes [19]. The PCI group comprised patients who were enrolled the day after PCI.

2.3 Inclusion and exclusion criteria

The inclusion criteria were as follows: (i) participants must have a diagnosis of CHD according to the aforementioned criteria; (ii) completion of CAG was required; (iii) participants must be aged between 18 and 85 years; (iv) participants voluntarily signed an informed consent form after receiving a comprehensive explanation of the study's objectives, procedures, potential risks, and benefits. The exclusion criteria were as follows: (i) pregnancy or breastfeeding; (ii) serious primary diseases, including malignant tumors; (iii) severe mental disorders, alcoholism, or drug abuse. To reduce potential effects on tongue characteristics, participants wearing braces or dentures were excluded from the study. Participants wearing facial makeup were also excluded.

2.4 Collection and analysis of tongue and facial features

Researchers who had received professional acquisition training at the Intelligent Processing Laboratory of Traditional Chinese Medicine Diagnostic Information, Shanghai University of Traditional Chinese Medicine, used the self-developed TFDA-1 tongue and face diagnosis instrument (Equipment No. ER17005-201810-41/50) to acquire images of the tongue and lips. The TFDA-1, a registered medical device, has been widely used in clinical settings to collect tongue and facial images. Its D50 light source provides high stability and excellent color reproduction. The device also has a lower jaw rest that ensures a standardized distance between the tongue or lip and the lens, minimizing distortion of the digital image, as demonstrated in extant studies [20, 21]. Before image acquisition, the instrument was disinfected with alcohol-soaked cotton balls, and researchers ensured that participants maintained neutral facial expressions, arrived after fasting, and had clean mouths and tongues, without foreign objects or discoloration. Participants were instructed to sit comfortably, resting their lower jaw on the mandibular support. First, they were asked to slightly close their eyes to align their lips for image capture. Then, they opened their mouths and extended their tongues to expose the tongue surface for imaging fully. Finally, participants were instructed to gently place the tip of their tongues against the maxillary incisal margin, thereby completely exposing the sublingual veins (SVs) for image acquisition.

This study used the TDAS, developed by the Smart Diagnosis Technology Research Team at Shanghai University of Traditional Chinese Medicine, to extract color features from the tongue and lips. The system automatically identifies the center points of the upper and lower lips and extracts relevant tongue components. Using a split-and-merge algorithm combined with a color threshold method, the system distinguishes between the tongue body (TB) and the tongue coating (TC) on the tongue surface. It differentiates SVs from other structures on the ventral surface and calculates their corresponding color values. The tongue and lip color indices were derived from the Lab color space, with the prefix “TB-” indicating the tongue body, “TC-” indicating the tongue coating, “SV-” indicating sublingual veins, and “lip-” indicating the lip body. A schematic diagram of the Lab color space is presented in Figure 1, and the meanings of the parameters are detailed as follows. (i) TB/TC/SV/lip-L: higher L values indicate a brighter color, whereas lower values indicate a darker color. (ii) TB/TC/SV/lip-a: the a value represents the red-green axis; higher values indicate a redder color, whereas lower values indicate a greener color. (iii) TB/TC/SV/lip-b: the b value represents the yellow-blue axis; higher values indicate a more yellow color, whereas lower values indicate a bluer color.

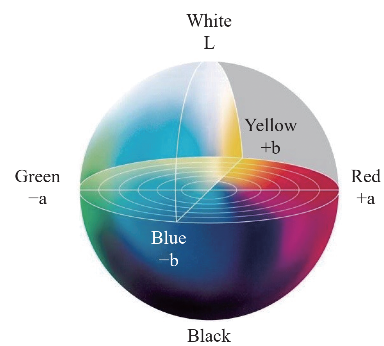

Figure 1 Schematic diagram of the Lab color space

2.5 Principal component analysis (PCA) for feature reduction and collinearity analysis

To identify the core indicators from the extensive information, this study used PCA for feature dimensionality reduction [22]. An orthogonal transformation was used to convert d-dimensional data into d'-dimensional data (where $d' < d$), while retaining as much information as possible. Linear dependence may exist in a certain linear dependence among the d-dimensional data, whereas the d'-dimensional data lack such linear dependence [23]. PCA decomposes the total variance of the m original indicators into the sum of the variances of m uncorrelated composite indicators, thereby maximizing the variance of the first principal component, denoted as λ_1. The contribution ratio of the first principal component is defined as the ratio of the variance of the first principal component λ_1 to the total variance, expressed as follows:

$$\lambda_1 / \sum_{i=1}^{m} \lambda_i \tag{1}$$

A larger ratio indicates a greater capacity of the indicator to synthesize the original indicators.

The contribution rate of the i-th principal component Z_i is expressed as follows:

$$\frac{\lambda_i}{\sum_{i}^{m}\lambda_i} = \frac{\lambda_i}{m}\ (k = 1, 2, \ldots, m) \tag{2}$$

The cumulative contribution rate of the first k principal components is expressed as follows:

$$\sum_{i=1}^{k}\frac{\lambda_i}{m}\ (k \leqslant m) \tag{3}$$

Principal components were retained according to the following principles. (i) The number of principal components was determined using the scree plot. If the inflection point of the scree plot occurs at the k-th principal component, the first k principal components were retained. (ii) The first k principal components were retained when the cumulative contribution rate exceeds 60%.

The factor loading q_{ij}, which represents the correlation coefficient between the i-th principal component and the j-th original indicator X_j, indicates the strength and direction of the association between the principal component Z_i and the original indicator X_i. The factor loading was calculated as the product of the square root $\sqrt{\lambda_i}$ of the eigenvalue of the i-th principal component Z_i and the coefficient α_{ij} of the j-th original indicator X_j, expressed as follows:

$$q_{ij} = \sqrt{\lambda_i \alpha_{ij}} \tag{4}$$

The rotated component matrix was extracted to obtain the absolute value of the loading coefficient between the common factor (principal component) and the original indicator. A larger absolute value indicated that the corresponding indicator is more representative of the original data features.

Pearson correlation coefficients were then used to assess collinearity. An absolute correlation coefficient greater than 0.8 between two variables indicates potential collinearity issues [24], and the corresponding indicators were excluded.

2.6 Machine learning models

This study used several common machine learning algorithms, including random forests, LightGBM, decision trees, and naive Bayes, to develop classification models for the coronary artery stenosis severity. Decision trees are traditional algorithms for classification and regression tasks; they divide data based on training data and feature attributes for effective classification or prediction [25, 26]. Random forests, which are ensemble learning algorithms based on decision trees, construct multiple trees and merge their results, with randomness helping to prevent overfitting [27, 28]. LightGBM is an efficient gradient-boosting decision tree framework based on histogram-based algorithms. Using a leaf-wise growth strategy and gradient-based one-sided sampling significantly improves training speed and reduces memory usage while maintaining high accuracy [29]. Naive Bayes classification, grounded in Bayes' theorem, classifies samples by calculating the probability that a sample belongs to a given class [30].

The R programming language (version 4.2.1) was used for modeling. To address missing values and outliers, features with more than 20% missing values were excluded. The continuous variables in the remaining samples were normalized using Z scores, and the final dataset was randomly divided into training and test sets at a 7 : 3 ratio. For each model, the hyperparameter set that maximized the area under the receiver operating characteristic (ROC) curve (AUC) on the training set was selected using a Bayesian optimizer to support optimal performance and prediction on the test set. Model performance was evaluated using accuracy, sensitivity, specificity, F1 score, precision, and AUC. To improve the interpretability of the machine learning model, this study employed the SHapley Additive exPlanations (SHAP) interpreter to visualize the classification results. Decision curve analysis (DCA) was also performed to evaluate the clinical utility of the models [31, 32]. True positive (TP) is the number of positive samples which are correctly predicted. True negative (TN) is the number of negative samples which are correctly predicted. False positive (FP) denotes the number of negative samples which are predicted to be positive. False negative (FN) is the number of positive samples predicted to be negative. The formulas for sensitivity, specificity, F1 score, precision, and accuracy are as follows.

$$\text{Sensitivity} = \frac{\text{TP}}{\text{TP} + \text{FN}} \tag{5}$$

$$\text{Specificity} = \frac{\text{TN}}{\text{TN} + \text{FP}} \tag{6}$$

$$\text{F1 score} = \frac{2 \times \text{Precision} \times \text{Sensitivity}}{\text{Precision} + \text{Sensitivity}} \tag{7}$$

$$\text{Precision} = \frac{\text{TP}}{\text{TP} + \text{FP}} \tag{8}$$

$$\text{Accuracy} = \frac{\text{TP} + \text{TN}}{\text{TP} + \text{TN} + \text{FP} + \text{FN}} \tag{9}$$

2.7 PLS-SEM

PLS-SEM shows how latent variables can be represented as a series of associations among observed variables. It consists of a structural model (the internal model) and a measurement model (the external model). The structural model describes the relationships among latent variables, and the measurement model describes the relationships between latent variables and their corresponding observed variables [33]. In this study, "myocardial biomarkers" "tongue body" "tongue coating" and "sublingual veins" were classified as latent variables, each with specific indicators. For example, myocardial function can be evaluated using creatine kinase-myocardial band (CK-MB), CK, and myoglobin (MYO), while tongue characteristics can be assessed through tongue color space parameters. These specific quantitative indicators are referred to as observed variables.

To investigate the intrinsic association and direction, this study focuses on patients after PCI. SmartPLS version 4.1.1.6 was used to construct and validate a conceptual model linking myocardial biomarkers and tongue characteristics. The study was conducted in two phases. In the first phase, the construct reliability and validity were evaluated. More specifically, Cronbach's alpha, average variance extracted (AVE), and composite reliability (CR) were used to assess the reliability, convergent validity, and composite reliability of the reflective measurement model [34]. In the second phase, statistical significance and path coefficients were calculated using bootstrapping with 5 000 resamples. The overall flowchart for this study is shown in Figure 2.

2.8 Statistical analysis

SPSS 25.0 was used for data analysis. For continuous variables, multiple imputation by chained equations (MICE) was used to complete missing data. For categorical variables, the mode, defined as the value with the highest frequency, was used for imputation. Categorical data were reported as frequencies and percentages. Continuous data with normal distributions were presented as mean ± standard deviation (SD), whereas non-normally distributed continuous data were described using medians and interquartile ranges (IQRs). Group comparisons were performed using the Chi-square test for categorical variables and the Kruskal-Wallis H test for continuous variables, with the Bonferroni correction for multiple testing. A two-tailed $P < 0.05$ was considered statistically significant for the comparisons.

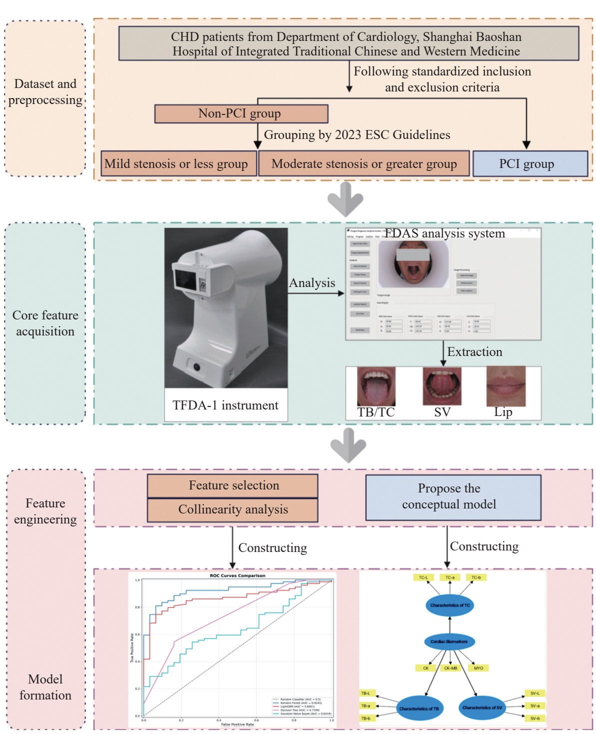

Figure 2 Overall flowchart of data collection, processing, and modeling

3 Results

3.1 Demographic information of patients with CHD

The study ultimately included 459 patients diagnosed with CHD, who were divided into two groups: a PCI group consisting of 95 patients and a non-PCI group comprising 364 patients. The non-PCI group was further categorized into a subgroup with mild stenosis or less (104 patients) and a subgroup with moderate stenosis or greater (260 patients). As shown in Table 1, demographic characteristics differed significantly among the three groups concerning sex ($P < 0.001$) and smoking status ($P = 0.003$). Specifically, women accounted for 62.50% of patients with mild stenosis or less, while men predominated in both the moderate stenosis or greater and PCI groups. Furthermore, nonsmokers outnumbered smokers across all three groups. For laboratory indicators, the PCI group had significantly higher triglycerides (TG) and high-density lipoprotein (HDL) than the non-PCI group ($P = 0.036$ and $P = 0.002$, respectively).

3.2 TCM observation features of patients with CHD

As shown in Table 2, comparisons among the three groups, the PCI group had significantly higher TB-L ($P < 0.05$), TB-a ($P < 0.01$), and TB-b ($P < 0.001$) in terms of tongue surface features, as well as significantly higher TC-a ($P < 0.01$) and TC-b values ($P < 0.001$). For SV features, the PCI group had lower SV-a values than the mild stenosis or less group ($P < 0.01$) and lower SV-b values than the moderate stenosis or greater group ($P < 0.05$). Concerning lip color values, no statistically significant differences were observed between the groups ($P > 0.05$). From a color-space analysis perspective, the SV features showed a more pronounced blue-green tendency in the PCI group. In contrast, the tongue surface features indicated a brighter, redder tongue color in the PCI group compared with the other two groups.

3.3 Variable selection

3.3.1 PCA feature reduction The cumulative variance explained by the seven common factors was 61.439%. According to the principle described above, PC1, PC2, PC3, PC4, PC5, PC6, and PC7 were able to represent the original indicators, collectively retaining 61.439% of the original information with a favorable contribution rate

Table 1 General characteristics of included CHD patients (n = 459)

Variable		Non-PCI group (n = 364)		PCI group (n = 95)	Statistical value	P value
		Mild stenosis or less (n = 104)	Moderate stenosis or greater (n = 260)			
Age (mean ± SD)		67.51 ± 10.17	67.88 ± 9.50	68.24 ± 9.30	H = 0.228	0.892[a]
BMI (mean ± SD)		24.84 ± 3.19	24.59 ± 3.33	24.65 ± 3.64	H = 0.530	0.767[a]
Sex [n (%)]	Male	39 (37.50)	158 (60.77)	55 (57.89)	χ^2 = 16.679	< 0.001[b]
	Female	65 (62.50)	102 (39.23)	40 (42.11)		
Smoking [n (%)]	Smoker	22 (21.15)	102 (39.23)	37 (38.95)	χ^2 = 11.448	0.003[b]
	Nonsmoker	82 (78.85)	158 (60.77)	58 (61.05)		
Drinking [n (%)]	Drinking	16 (15.38)	60 (23.08)	24 (25.26)	χ^2 = 3.429	0.180[b]
	Nondrinking	88 (84.62)	200 (76.92)	71 (74.74)		
Medical history [n (%)]	Hypertension	44 (42.31)	115 (44.23)	41 (43.16)	χ^2 = 2.273	0.893[b]
	Diabetes	7 (6.73)	20 (7.69)	7 (7.37)		
	Both of the above	25 (24.04)	73 (28.08)	25 (26.32)		
	None	28 (26.92)	52 (20.00)	22 (23.16)		
Stent implantation [n (%)]	Yes	20 (19.23)	72 (27.69)	29 (30.53)	χ^2 = 3.810	0.149[b]
	No	84 (80.77)	188 (72.31)	66 (69.47)		
NYHA classification [n (%)]	Class I	20 (19.23)	47 (18.08)	24 (25.26)	χ^2 = 8.024	0.236[b]
	Class II	57 (54.81)	121 (46.54)	40 (42.11)		
	Class III	27 (25.96)	87 (33.46)	28 (29.47)		
	Class IV	0 (0.00)	5 (1.92)	3 (3.16)		
Coagulation (mean ± SD)	FIB	2.98 ± 0.68	3.16 ± 0.85	3.23 ± 0.99	H = 2.994	0.224[a]
	PT	17.42 ± 1.61	17.47 ± 1.71	18.06 ± 3.16	H = 3.305	0.192[a]
	D-D	0.39 ± 0.28	0.41 ± 0.30	0.91 ± 0.39	H = 2.741	0.254[a]
	AT3	93.48 ± 13.28	91.62 ± 11.87	91.51 ± 11.76	H = 2.121	0.346[a]
Lipid metabolism (mean ± SD)	Total cholesterol	4.21 ± 1.07	4.07 ± 1.16	4.29 ± 1.20	H = 2.517	0.284[a]
	TG	1.50 ± 0.74	1.55 ± 0.68	1.89 ± 0.75	H = 6.653	0.036[a]
	HDL	1.16 ± 0.27	1.06 ± 0.24	1.57 ± 0.58	H = 2.422	0.002[a]
	LDL	2.51 ± 0.76	2.47 ± 0.82	2.58 ± 0.81	H = 1.417	0.492[a]
Myocardial markers (mean ± SD)	CK	84.37 ± 8.34	89.42 ± 3.21	98.21 ± 3.34	H = 0.324	0.850[a]
	CK-MB	1.43 ± 0.93	1.49 ± 1.02	1.76 ± 1.06	H = 1.163	0.559[a]
	MYO	45.60 ± 2.78	46.74 ± 2.65	55.38 ± 5.75	H = 0.855	0.652[a]

a, Kruskal-Wallis H test. b, Chi-square test. NYHA, New York Heart Association. PT, Prothrombin Time. D-D, D-Dimer. AT3, antithrombin III. LDL, low-density lipoprotein.

Table 2 Statistical analysis of tongue and lip indices [median (P25, P75)]

Domain	Index	Non-PCI group (n = 364)		PCI group (n = 95)
		Mild stenosis or less (n = 104)	Moderate stenosis or greater (n = 260)	
TB	TB-L	37.12 (34.35 – 39.64)	37.45 (35.55 – 39.02)	38.19 (36.14 – 40.04)*
	TB-a	22.90 (20.42 – 24.55)	23.20 (21.10 – 24.55)	24.31 (21.87 – 26.49)**▲▲
	TB-b	8.26 (7.12 – 9.95)	8.15 (7.18 – 9.80)	9.36 (8.03 – 10.97)**▲▲▲
TC	TC-L	34.71 (31.81 – 37.81)	34.91 (32.27 – 37.84)	35.96 (31.77 – 38.63)
	TC-a	17.19 (14.97 – 18.49)	17.18 (15.55 – 19.02)	18.03 (16.42 – 20.02)**▲
	TC-b	6.03 (5.04 – 7.61)	6.24 (5.00 – 7.52)	7.05 (5.97 – 8.50)**▲▲▲
SV	SV-L	50.03 (43.55 – 56.00)	51.02 (43.10 – 57.69)	52.56 (45.32 – 60.15)
	SV-a	22.05 (19.31 – 25.60)	21.05 (17.79 – 24.72)	20.18 (17.54 – 22.08)**
	SV-b	8.30 (5.98 – 11.36)	8.60 (6.08 – 10.75)	7.03 (5.44 – 9.15)▲
Lip	Lip-L	38.24 (37.23 – 39.40)	38.15 (37.03 – 39.24)	/
	Lip-a	23.63 (22.02 – 25.10)	23.45 (22.00 – 24.97)	/
	Lip-b	14.63 (13.17 – 15.68)	14.62 (13.58 – 15.96)	/

*P < 0.05 and **P < 0.01, compared with the mild stenosis or less group. ▲P < 0.05, ▲▲P < 0.01, and ▲▲▲P < 0.001, compared with the moderate stenosis or greater group. "/" indicates no data were available.

(Figure 3 and Table 3). Analysis of the factor loadings and the extraction of the rotated component matrix showed that the variables best reflecting the characteristics of the original data were age, SV-a, SV-b, total cholesterol, low-density lipoprotein (LDL), CK-MB, CK, TB-b, TC-a, TC-b, lip-L, and lip-b (Table 4).

3.3.2 Collinearity analysis As shown in Figure 4, the four variables (total cholesterol, LDL, TB-b, and TC-b) showed multicollinearity. The correlation coefficient between the lipid metabolism indicators total cholesterol and LDL was 0.93, whilst the correlation coefficient between the tongue indicators TC-b and TB-b was 0.89. Therefore, these four variables were excluded from the machine learning models.

3.4 Machine learning models for predicting coronary artery stenosis severity

After age, SV-a, SV-b, CK, CK-MB, TC-a, lip-L, and lip-b were incorporated as input variables into the machine learning models. The random forest algorithm showed the best overall performance, with the highest AUC (0.924), F1 score (0.839), precision (0.807), and accuracy (0.864). LightGBM also performed well with an AUC of 0.866, followed by the decision tree and naive Bayes (Figure 5 and Table 5).

The SHAP interpreter was used to visually present the selected variables and to show the positive and negative influences of each feature on the samples. Figure 6 displays the mean absolute SHAP values of each feature. Among the variables with the greatest impact on the coronary artery stenosis severity, SV-a had the strongest influence, followed by SV-b. TC-a and lip-L also affected the degree of coronary artery stenosis.

DCA indicated that all machine learning models had clinical utility (Figure 7). Comparison of the net benefit values of the models at critical threshold points (Table 6) showed that LightGBM and the random forest model consistently maintained high net benefit across the entire threshold interval, indicating their generalizability. Specifically, at the clinically relevant threshold of 0.2, the net benefit of LightGBM was 0.345, suggesting that model-guided decision-making in the target population was superior to blind intervention, as evidenced by a net benefit of 0.164 for blind intervention. Therefore, LightGBM and random forest are recommended as the core methods for clinical decision support systems.

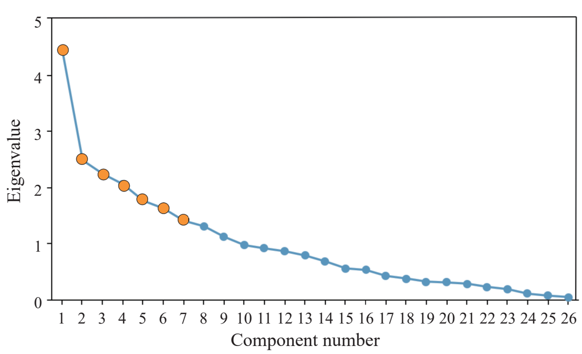

Figure 3 Scree plot of the components via PCA

Steeper slopes indicate larger eigenvalues and greater information content.

Table 3 Eigenvalues and variance contribution rates for the seven principal components via PCA

PC	Eigenvalue	Cumulative contribution rate (%)
PC1	4.432	17.047
PC2	2.477	26.576
PC3	2.235	35.172
PC4	2.051	43.059
PC5	1.757	49.818
PC6	1.620	56.049
PC7	1.401	61.439

Table 4 Rotated component matrix using the varimax method

Variable	Absolute value of factor loadings							Communality
	PC1	PC2	PC3	PC4	PC5	PC6	PC7	
Age	– 0.061	– 0.062	– 0.139	0.009	0.066	0.053	0.822	0.710
SV-a	0.025	– 0.010	– 0.013	0.017	0.003	0.896	– 0.014	0.807
SV-b	0.020	– 0.006	0.021	0.011	0.072	0.883	– 0.028	0.803
Total cholesterol	– 0.021	0.967	– 0.032	– 0.029	0.012	– 0.032	0.056	0.942
LDL	0.017	0.930	0.009	– 0.013	– 0.039	– 0.012	0.033	0.869
CK-MB	– 0.062	0.039	– 0.155	0.836	– 0.018	0.015	0.078	0.742
CK	– 0.036	– 0.009	– 0.012	0.852	– 0.032	0.051	– 0.236	0.798
TB-b	0.277	0.014	0.159	– 0.029	0.880	0.052	0.081	0.893
TC-a	0.142	0.054	0.823	0.004	0.164	0.126	– 0.128	0.765
TC-b	0.179	0.018	0.122	– 0.013	0.885	0.013	0.044	0.848
Lip-L	0.804	0.006	0.173	– 0.068	0.023	0.001	0.158	0.718
Lip-b	0.810	0.031	0.033	0.051	0.318	0.007	– 0.109	0.786

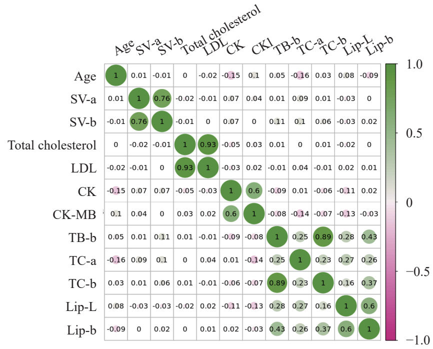

Figure 4 Pearson correlation plot of variables

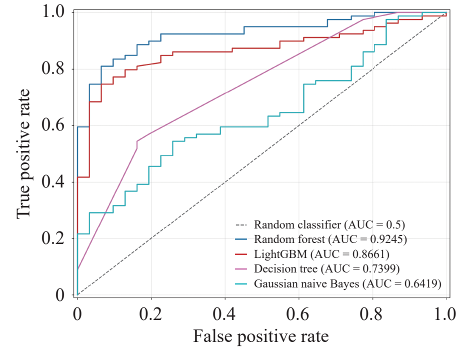

Figure 5 AUC comparison of machine learning models

Table 5 Evaluation of the machine learning models performance

Model	Sensitivity	Specificity	Precision	F1 score	Accuracy	AUC
Random forest	0.873	0.839	0.807	0.839	0.864	0.924
LightGBM	0.759	0.903	0.805	0.782	0.800	0.866
Decision tree	0.519	0.839	0.717	0.602	0.609	0.740
Naive Bayes	0.937	0.161	0.374	0.535	0.718	0.642

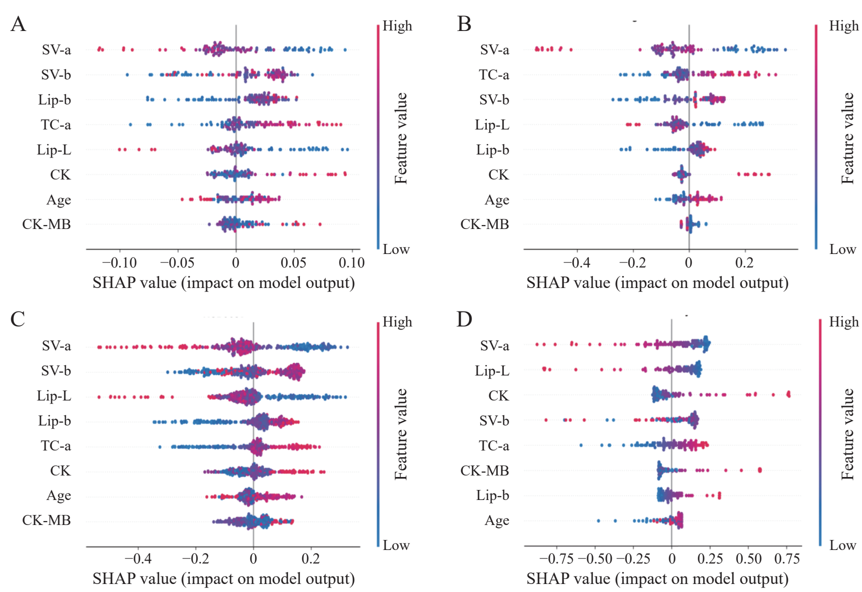

Figure 6 SHAP explanations of the machine learning models

A, random forest. B, LightGBM. C, decision tree. D, naive Bayes.

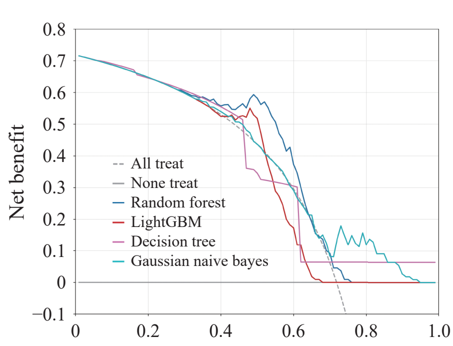

Figure 7 DCA of all machine learning models

3.5 The association chain between cardiac markers and tongue features after PCI using PLS-SEM

First, a conceptual model linking myocardial biomarkers to tongue features was constructed using PLS-SEM (Figure 8). Then, the performance of the PLS-SEM external model was analyzed to validate the chain between myocardial biomarkers and tongue after PCI. A Cronbach's alpha of 0.6 or higher indicates satisfactory reliability of the external model. Additionally, an AVE of 0.5 or higher and a CR of 0.7 or higher indicated good convergent validity and composite reliability of the reflective model. Adjusted

R^2 values of endogenous constructs exceeded 0.5, indicating that the model had good explanatory power (Table 7).

As shown in Table 8, the path relationships among latent variables indicated that the relationships between myocardial biomarkers and TB (P = 0.025) and between myocardial biomarkers and TC (P = 0.012) were established. This finding indicates that post-PCI myocardial biomarkers directly influence both TB and TC.

Table 6 Net benefit values at key threshold points across classifiers (treat strategies)

Threshold probability	Random forest	LightGBM	Decision tree	Naive Bayes	All treat strategy
0.1	0.326	0.341	0.289	0.257	0.082
0.2	0.318	0.345	0.281	0.249	0.164
0.3	0.305	0.322	0.268	0.236	0.246

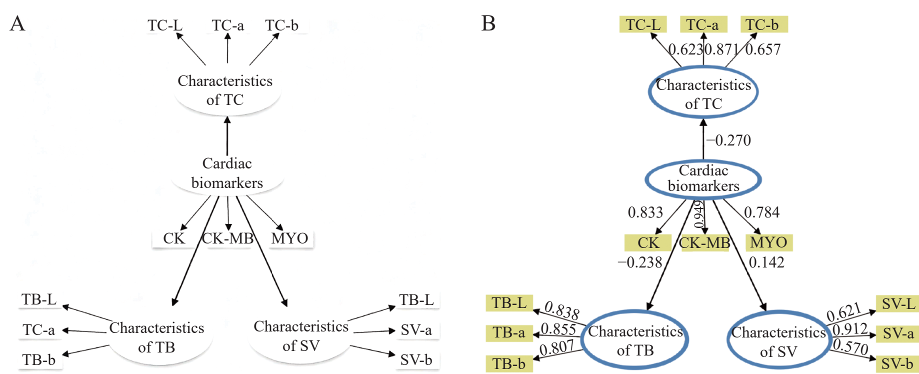

Figure 8 PLS-SEM for estimating the association between myocardial markers and tongue features

A, PLS-SEM conceptual model. B, PLS-SEM validation model. Rectangles indicate observed variables, and ovals indicate latent variables. Arrows connecting the ovals and the numbers indicate the paths and path coefficients between the latent variables.

Table 7 PLS-SEM model structure and the assessment of its performance

Construct	Type	Item	Loading	Cronbach's alpha	AVE	CR	Adjusted R^2
Myocardial biomarkers	Reflective	CK	0.838	0.86	0.74	0.90	/
		CK-MB	0.949				
		MYO	0.784				
Characteristics of TB	Reflective	TB-L	0.838	0.78	0.70	0.87	0.72
		TB-a	0.855				
		TB-b	0.807				
Characteristics of TC	Reflective	TC-L	0.623	0.60	0.53	0.77	0.61
		TC-a	0.871				
		TC-b	0.657				
Characteristics of SV	Reflective	SV-L	0.621	0.73	0.51	0.50	0.55
		SV-a	0.912				
		SV-b	0.570				

"/" indicates no data were available. Myocardial biomarkers, as exogenous latent variables, do not have an R^2 value.

Table 8 The path coefficients and statistical significance in PLS-SEM model

Path	Coefficient	Bootstrapped sample mean	t	P value	Decision
Myocardial markers → characteristics of SV	0.142	0.055 (0.202)	0.702	0.483	Rejected
Myocardial markers → characteristics of TB	– 0.238	– 0.261 (0.106)	2.239	0.025	Supported
Myocardial markers → characteristics of TC	– 0.270	– 0.277 (0.107)	2.522	0.012	Supported

4 Discussion

The association between TCM observation diagnosis and cardiovascular health was first documented in the *Huangdi Neijing* (《黄帝内经》, *Inner Canon of Huangdi*), which states that "the heart opens its orifice to the tongue" [7]. This phrase suggests that the tongue's characteristics can reflect cardiac function. The observation that "in heart disease, the tongue is curled and short, with reddened cheeks" indicates a connection between the heart and facial diagnostic features in pathological states. TCM posits that blood stasis obstructing the coronary vessels is a primary pathological mechanism underlying CHD [35]. Additionally, "the lips are the glory of the spleen; the spleen governs blood, and the heart controls blood", suggests that changes in lip color can reflect visceral disorders and the circulation of heart blood [36, 37]. This study employed the independently developed TFDA-1 tongue and face diagnosis instrument and the TDAS analysis system to facilitate a convenient, non-invasive, and precise intelligent facial visual diagnosis, and to explore the association between color parameters and CHD, thereby offering new possibilities for CHD risk assessment and proactive health management.

4.1 Analysis of TCM visual diagnostic features in CHD patients

In comparisons of visual diagnostic features within CHD subgroups, this study found that the PCI group showed a more pronounced bluish-green tendency (SV-b) in SVs, indicating persistent blood stasis [38]. This observation is consistent with the common clinical manifestations of microcirculation disorders that commonly occur after post-PCI conditions [39, 40]. The SV provides an important window for assessing blood circulation [41, 42] and shows a closer association with microcirculation disorders than the tongue surface [43, 44]. This finding provides objective evidence for identifying the progression and prognosis of CHD from a TCM perspective.

4.2 Analysis of the results from the coronary stenosis assessment model

Recent study has increasingly used non-invasive indicators to develop early warning models for CHD. In studies predicting the risk of major adverse cardiovascular events after PCI, a model that integrates clinical indicators with Agatston scores achieved an AUC of 0.857 [45]. Another study evaluating the predictive value of electrocardiographic signal characteristics for cardiovascular risk found that including electrocardiographic signals improved the C-index of the predictive model from 0.84 to 0.85 [46]. The present study used various feature selection methods to identify relevant variables and constructed machine learning models to evaluate the risk of coronary artery stenosis. The random forest model performed best, with an AUC of 0.924, and its decision curve analysis yielded a favourable net benefit of 0.326. Therefore, it is recommended for clinical decision-making. This performance was better than that reported in similar studies, supporting the value of multimodal features derived from non-invasive TCM methods in the clinical management of CHD.

For visualization of machine learning results, variable importance analysis using the SHAP method showed that SV-a had the strongest impact on coronary artery stenosis, followed by SV-b. Previous research has identified purplish-red sublingual veins as a key manifestation of blood stasis associated with CHD [47], supporting the conclusion of the current study that the SV-a and SV-b indices significantly influence the severity of coronary artery stenosis. Individuals with abnormalities in SV-a and SV-b indicators may therefore warrant particular attention, because early intervention in these populations may help reduce disease risk.

4.3 Exploratory analysis of the association chain between tongue features and cardiac biomarkers

This study applies the PLS-SEM model to explore the association between myocardial biomarkers and tongue features following PCI. It supports directed acyclic graph relationships [48], specifically myocardial biomarkers → TB and myocardial biomarkers → TC. Myocardial biomarkers are important indicators for assessing adverse events in CHD, such as myocardial infarction [49]. The findings of this study show that both TB and TC are closely associated with these indicators. This exploratory approach may support post-PCI assessment in CHD through convenient, non-invasive tongue diagnosis. It may help clinicians make timely treatment adjustments, prevent adverse coronary events, and reduce health care costs for patients.

4.4 Limitations and future prospects

This study has several limitations. First, all data were collected from a single center, which limits the representativeness of the sample in terms of geographical location and clinical setting, and may affect the generalizability of the conclusions. Second, the machine learning model developed in this study is limited to assessing the severity of coronary artery stenosis in patients with a confirmed diagnosis of CHD; its value in distinguishing other cardiovascular diseases characterised by blood stasis will be verified in future generalisation trials. Finally, while this study employed PLS-SEM to examine the association between tongue characteristics and myocardial biomarkers and to validate the proposed causal chain, the model's reliability, as indicated by the CR value, warrants further improvement. Future research should integrate multimodal clinical indicators, include multi-disease cohorts such as chronic heart failure and cerebral infarction, adopt multiclass model strategies to enhance the disease-specific assessment, and conduct prospective, multicenter external validation studies.

5 Conclusion

The machine learning models for coronary artery stenosis risk warning showed that the random forest algorithm performed better overall, and tongue and facial features observed in TCM diagnosis were useful for assessing the degree of coronary artery stenosis. A conceptual model linking myocardial biomarkers with tongue features was developed for patients undergoing PCI. Internal and external model validation confirmed the association chains: myocardial biomarkers → TB and myocardial biomarkers → TC. Overall, this study, grounded in modernized TCM visual diagnosis techniques, provides evidence for developing tools to assess the severity of coronary artery stenosis in patients with CHD, and may support proactive, full-cycle health management in CHD patients.

Fundings

National Science and Technology Major Project of China (2025ZD0545000), Shanghai Science and Technology Committee Rising-Star Program (24YF2746000), and Research Project of Shanghai Municipal Health Commission (2024QN018).

Ethical statement

This study was conducted in accordance with the Declaration of Helsinki. It was approved by the Ethics Committee of Shuguang Hospital Affiliated to Shanghai University of Traditional Chinese Medicine (Approval No. 2023-2-5-04), and was registered in the Chinese Clinical Trial Registry (ChiCTR1900026008). All participants provided written informed consent.

Acknowledgements

The authors are especially thankful for the positive support received from Shanghai Baoshan Hospital of Integrated Traditional Chinese and Western Medicine.

Author contributions

Yu Wang: conceptualization, data curation, formal analysis, funding acquisition, methodology, and writing. Pengcheng Ding: formal analysis, methodology, and writing – review & editing. Zhentao Li: formal analysis, methodology, and writing – review & editing. Jiyu Zhang: data curation and investigation. Liping Tu: methodology and resources. Jijie Xu: data curation, methodology, project administration, resources, and supervision. Jiatuo Xu: conceptualization, funding acquisition, project administration, resources, and supervision. All authors approved the submission and take responsibility for this manuscript.

Competing interests

Jiatuo Xu is an editorial board member for *Digital Chinese Medicine* and was not involved in the editorial review or the decision to publish this article. Yu Wang is a postdoctoral researcher jointly supervised by Shanghai University of Traditional Chinese Medicine and Wuhu Shengmeifu Technology Co., Ltd., and has no financial or non-financial conflicts of interest, such as research funding, employment, shareholdings or patents, with either of these institutions. All authors declare no competing interests.

References

[1] LIU YF, ZHANG XY, WAN WL, et al. Two new stenosis detection methods of coronary angiograms. International Journal of Computer Assisted Radiology and Surgery, 2022, 17(3): 521–530.

[2] SEIFFERT M, OJEDA F, MÜLLERLEILE K, et al. Reducing radiation exposure during invasive coronary angiography and percutaneous coronary interventions implementing a simple four-step protocol. Clinical Research in Cardiology, 2015, 104(6): 500–506.

[3] American College of Radiology, Society of Cardiovascular Computed Tomography, Society for Cardiovascular Magnetic Resonance, et al. ACCF/ACR/SCCT/SCMR/ASNC/NASCI/SCAI/SIR 2006 appropriateness criteria for cardiac computed tomography and cardiac magnetic resonance imaging. A report of the American College of Cardiology Foundation Quality Strategic Directions Committee Appropriateness Criteria Working Group. Journal of the American College of Radiology, 2006, 3(10): 751–771.

[4] HU X, ZHANG J, YANG S, et al. Angiography-derived fractional flow reserve versus intravascular ultrasound to guide percutaneous coronary intervention in patients with coronary artery disease (FLAVOUR II): a multicentre, randomised, non-inferiority trial. Lancet, 2025, 405(10488): 1491–1504.

[5] SCHNITZLER GR, KANG H, FANG S, et al. Convergence of coronary artery disease genes onto endothelial cell programs. Nature, 2024, 626(8000): 799–807.

[6] KHAN SS, GREENLAND P, HAYMAN LL, et al. Criteria to assess the predictive and clinical utility of novel models, biomarkers, and tools for risk of cardiovascular disease: a scientific statement from the American heart association. Circulation, 2026, 153(11): 953–970.

[7] SUN X, REN H. Analysis of the Heart's body opening in the *Inner Canon of Huangdi*. Journal of Basic Chinese Medicine, 2018, 24(7): 873–874.

[8] NAKAJIMA K, MINAMI T, TANABE HC, et al. Facial color processing in the face-selective regions: an fMRI study. Human Brain Mapping, 2014, 35(9): 4958–4964.

[9] SUN GH, NAKAYAMA Y, DAGDANPUREV S, et al. Remote sensing of multiple vital signs using a CMOS camera-equipped

infrared thermography system and its clinical application in rapidly screening patients with suspected infectious diseases. International Journal of Infectious Diseases, 2017, 55: 113–117.
[10] ZHANG JY, XU JT, TU LP, et al. A non-invasive prediction model for coronary artery stenosis severity based on multimodal data. Frontiers in Physiology, 2025, 16: 1592593.
[11] ZHANG JY, XU JT, TU LP, et al. Risk assessment of coronary artery occlusion based on integrated Chinese and western medicine data. Digital Chinese Medicine, 2024, 7(4): 419–428.
[12] LI JY, XIONG DQ, HONG LX, et al. Tongue color parameters in predicting the degree of coronary stenosis: a retrospective cohort study of 282 patients with coronary angiography. Frontiers in Cardiovascular Medicine, 2024, 11: 1436278.
[13] CHEN L. Relationship between manifestations of tongue, lingual hemodynamics and heart function in patients with dilated cardiomyopathy. Chengdu: Sichuan University, 2006.
[14] CNEN J, LI N, ZHANG YF, et al. The formation mechanism of bluish tongue and its relationship with acute myocardial infarction. Asia-Pacific Traditional Medicine, 2022, 18(3): 192–195.
[15] ZHOU M, LI JY, LIM J, et al. A machine learning model integrating tongue image features and myocardial injury markers predicts major adverse cardiovascular events in patients with coronary heart disease. International Journal of General Medicine, 2025, 18: 3739–3765.
[16] DUAN JQ. Longitudinal study on tongue manifestation and therapeutic indicators in patients with phlegm and blood stasis syndrome after PCI for acute myocardial infarction. Shenyang: Liaoning University of Traditional Chinese Medicine, 2022.
[17] VISSEREN FLJ, MACH F, SMULDERS YM, et al. 2021 ESC Guidelines on Cardiovascular Disease Prevention in Clinical Practice. European Heart Journal, 2021, 42(34): 3227–3337.
[18] KNUUTI J, WIJNS W, SARASTE A, et al. 2019 ESC Guidelines for the Diagnosis and Management of Chronic Coronary syndromes. European Heart Journal, 2020, 41(3): 407–477.
[19] BYRNE R, COUGHLAN JJ, ROSSELLO X, et al. The 10 commandments for the 2023 ESC Guidelines for the Management of Acute Coronary Syndromes. European Heart Journal, 2024, 45(14): 1193–1195.
[20] WANG Y, LOU JD, LI J, et al. Relationship chains of subhealth physical examination indicators: a cross-sectional study using the PLS-SEM approach. Scientific Reports, 2023, 13: 13640.
[21] WANG Y, CHEN J, CHEN QC, et al. A new method for assessing chronic insomnia: machine learning-based fusion of TCM observation digital features. Digital Health, 2025, 11: 20552076251393331.
[22] JIAO W, HU XJ, TU LP, et al. Tongue color clustering and visual application based on 2D information. International Journal of Computer Assisted Radiology and Surgery, 2020, 15(2): 203–212.
[23] ZHOU ZH. Machine learning. 4th ed. Beijing: Tsinghua University Press, 2016.
[24] KIM JH. Multicollinearity and misleading statistical results. Korean Journal of Anesthesiology, 2019, 72(6): 558–569.
[25] PASHAEI E, OZEN M, AYDIN N. Improving medical diagnosis reliability using Boosted C5.0 decision tree empowered by Particle Swarm Optimization. 2015 37th Annual International Conference of the IEEE Engineering in Medicine and Biology Society (EMBC). IEEE, 2015: 7230-7233.
[26] WU SW, PAN Q, CHEN T. Research on diagnosis-related group grouping of inpatient medical expenditure in colorectal cancer patients based on a decision tree model. World Journal of Clinical Cases, 2020, 8(12): 2484–2493.
[27] CHEN WT, WANG Y, CAO GT, et al. A random forest model based classification scheme for neonatal amplitude-integrated EEG. BioMedical Engineering OnLine, 2014, 13(2): S4.
[28] SEO W, LEE YB, LEE S, et al. A machine-learning approach to predict postprandial hypoglycemia. BMC Medical Informatics and Decision Making, 2019, 19(1): 210.
[29] HAJIHOSSEINLOU M, MAGHSOUDI A, GHEZELBASH R. A novel scheme for mapping of MVT-type Pb-Zn prospectivity: LightGBM, a highly efficient gradient boosting decision tree machine learning algorithm. Natural Resources Research, 2023, 32(6): 2417–2438.
[30] ASAFU-ADJEI JK, BETENSKY RA. A pairwise Naïve Bayes approach to Bayesian classification. International Journal of Pattern Recognition and Artificial Intelligence, 2015, 29(7): 1550023.
[31] VICKERS AJ. Decision analysis for the evaluation of diagnostic tests, prediction models, and molecular markers. The American Statistician, 2008, 62(4): 314–320.
[32] VICKERS AJ, VAN CALSTER B, STEYERBERG EW. Net benefit approaches to the evaluation of prediction models, molecular markers, and diagnostic tests. BMJ, 2016, 352: i6.
[33] AVKIRAN NK. An in-depth discussion and illustration of partial least squares structural equation modeling in health care. Health Care Management Science, 2018, 21(3): 401–408.
[34] HAIR JF, SARSTEDT M, PIEPER TM, et al. The use of partial least squares structural equation modeling in strategic management research: a review of past practices and recommendations for future applications. Long Range Planning, 2012, 45(5/6): 320–340.
[35] MAO JY, NIU ZC, ZHANG BL. Analysis of literature on TCM syndrome characteristics of coronary heart disease in the past 40 years. Journal of Traditional Chinese Medicine, 2011, 52(11): 958–961.
[36] GUAN TH, FU HY, SHANG B. Study on the physiology of lips and the mechanism of abnormal lip color based on ancient Chinese medicine classics. Liaoning Journal of Traditional Chinese Medicine, 2026, 15(2): 1–13.
[37] ZHENG LL, LI XQ, LI FF, et al. Automatic classification of lip color in traditional Chinese medicine inspection based on support vector machine. Journal of Biomedical Engineering, 2011, 28(1): 7–11.
[38] CHIU CC, LAN CY, CHANG YH. Objective assessment of blood stasis using computerized inspection of sublingual veins. Computer Methods and Programs in Biomedicine, 2002, 69(1): 1–12.
[39] TANG N, LI KM, LI HR, et al. Advances in the diagnosis and management of post-percutaneous coronary intervention coronary microvascular dysfunction: insights into pathophysiology and metabolic risk interactions. World Journal of Cardiology, 2025, 17(2): 103950.
[40] NICOLAU AM, SILVA PG, MEJÍA HPG, et al. Molecular mechanisms of microvascular obstruction and dysfunction in percutaneous coronary interventions: from pathophysiology to therapeutics: a comprehensive review. International Journal of Molecular Sciences, 2025, 26(14): 6835.
[41] HEDSTRÖM L, ALBREKTSSON M, BERGH H. Is there a connection between sublingual varices and hypertension? BMC Oral Health, 2015, 15(1): 78.
[42] KHALILZADA M, DOGAN K, INCE C, et al. Sublingual microvascular changes in patients with cerebral small vessel disease. Stroke, 2011, 42(7): 2071–2073.

[43] MORITA A, MURAKAMI A, NOGUCHI K, et al. Combination image analysis of tongue color and sublingual vein improves the diagnostic accuracy of oketsu (blood stasis) in Kampo medicine. Frontiers in Medicine, 2022, 8: 790542.
[44] KAWANABE T, KAMARUDIN ND, OOI CY, et al. Quantification of tongue colour using machine learning in Kampo medicine. European Journal of Integrative Medicine, 2016, 8(6): 932–941.
[45] XING ZY, PAN HY, DING H, et al. Incremental value of non-gated chest CT coronary artery calcium score in predicting major adverse cardiovascular events by GRACE score after percutaneous coronary intervention in patients with acute coronary syndrome. Clinical Cardiology, 2026, 49: e70242.
[46] MAHDAVI M, KAZEMNEJAD A, ASOSHEH A, et al. Integrating ECG-derived features with conventional CVD risk models. Scientific Reports, 2025, 15: 39128.
[47] FENG Y, XU H, QU D, et al. Study on the tongue manifestations for the blood-stasis and toxin syndrome in the stable patients of coronary heart disease. Chinese Journal of Integrative Medicine, 2011, 17(5): 333–338.
[48] LIPSKY AM, GREENLAND S. Causal directed acyclic graphs. JAMA, 2022, 327(11): 1083.
[49] FRANCESCHINI N, KOPP JB, BARAC A, et al. Association of *APOL1* with heart failure with preserved ejection fraction in postmenopausal African American women. JAMA Cardiology, 2018, 3(8): 712.

(Editor-in-Charge Jie Deng)

中医面舌特征的冠状动脉阻塞预警及其与心肌标志物的关系研究

王瑜[a, b], 丁鹏程[c], 李镇涛[a], 张冀豫[a], 屠立平[d], 徐基杰[e*], 许家佗[a*]

a. 上海中医药大学中医学院, 上海 201203, 中国
b. 芜湖圣美孚科技有限公司生产技术部, 安徽 芜湖 241005, 中国
c. 安庆师范大学数字与智能健康研究中心, 安徽 安庆 246133, 中国
d. 上海中医药大学中医药人工智能学院, 上海 201203, 中国
e. 上海市宝山区中西医结合医院心血管内科, 上海 201999, 中国

【摘要】目的 本研究旨在探讨数字面舌望诊技术对冠心病患者冠状动脉阻塞程度的辅助评估价值，并探索数字舌象特征与心肌生物标志物之间的潜在关联。**方法** 采用 TFDA-1 面舌采集设备和 TDAS 分析系统对 2023 年 10 月 2 日至 2024 年 7 月 31 日在上海市宝山区中西医结合医院心血管内科就诊的冠心病患者进行智能化面舌望诊和分析。通过主成分分析和多重共线性分析筛选变量以构建随机森林、轻量级梯度提升机、决策树和朴素贝叶斯四种机器学习模型来预测冠状动脉阻塞程度，评估包括敏感性、特异性、精确度、F1 分数、准确度和受试者工作特征（ROC）曲线下面积（AUC）在内的模型性能指标，通过夏普利加性解释（SHAP）和决策曲线进行可视化分析。针对经皮冠状动脉介入治疗（PCI）术后患者，利用偏最小二乘结构方程模型（PLS-SEM）构建心肌标志物与舌象的概念关系模型并验证其有效性。**结果** 研究共纳入 459 例冠心病患者并将其划分为 PCI 组和非 PCI 组（非 PCI 组包含轻度阻塞及以下、中度阻塞及以上 2 个亚组）。在舌下络脉（SV）特征上，PCI 组的 SV-a 和 SV-b 显著更低（分别为 $P < 0.01$、$P < 0.05$）；在舌面特征上，PCI 组的舌质（TB）-L、TB-a 和 TB-b 显著更高（分别为 $P < 0.05$、$P < 0.01$、$P < 0.001$），舌苔（TC）-a 和 TC-b 也显著更高（分别为 $P < 0.01$、$P < 0.001$）。将变量年龄、SV-a、SV-b、肌酸激酶同工酶 MB 型（CK-MB）、CK、TC-a、lip-L、lip-b 纳入机器学习模型，性能评估显示，随机森林表现更佳，其 AUC 值达到 0.924，F1 分数 0.839，精确度 0.807，准确度 0.864，敏感性 0.873，特异性 0.839。此外，决策曲线分析表明，LightGBM 和随机森林均具有临床实用价值。PLS-SEM 模型显示心肌标志物→舌质、心肌标志物→舌苔的路径关系链是成立的（coefficient = – 0.238，$t = 2.239$，$P = 0.025$; coefficient = – 0.270，$t = 2.522$，$P = 0.012$)。**结论** 本研究构建了无创化冠心病冠状动脉阻塞预警模型，将 PLS-SEM 应用于 PCI 术后心肌标志物与舌象的关系研究，并验证了关系链的成立。将中医望诊与现代数字技术相结合，可为冠心病风险评估和健康管理提供支持。

【关键词】舌诊；面诊；冠心病；风险预警模型；偏最小二乘结构方程模型